A tetrahedral anvil apparatus for optical studies under high hydrostatic pressures

C D Clark and R J Wedlake†
J J Thomson Physical Laboratory, University of Reading, Berks.

Received 17 July 1972

Abstract A method of modifying a tetrahedral anvil apparatus to allow optical experiments to be performed under high pressures and at low temperatures is described. Solid samples with dimensions of 2 or 3 mm can be studied within the following ranges: 0–50 kbar, 100–300 K, 2000–8000 Å. The system is designed so that at least two pressure calibration points can be obtained during each experiment. A method of pressure calibration at low temperatures is described. Such pressure calibration checks are necessary because the pressure–load curves vary markedly with temperature and tetrahedron design. The apparatus has been used to measure the pressure dependence of the energies of zero-phonon absorption lines in diamond.

1 Apparatus

The tetrahedral anvil equipment, as developed by The National Physical Laboratory and described by Bradley (1969), is used as the basis for an optical high pressure apparatus. Schematic sections through the apparatus are shown in figure 1. The anvils labelled 1, 2, 3 and 4 are arranged tetrahedrally in a steel cone. Anvils 1 and 3 have stepped holes which run concentrically along the axes of the anvils, and emerge as 3·25 mm diameter holes at the centroid of the triangular anvil faces which are made of tungsten carbide. The holes are 6·35 mm diameter through the steel backing blocks. The holes in the anvils may be aligned by eye with the 9·53 mm diameter holes in the steel cone. An oversize pyrophyllite tetrahedron (side length 28·6 mm) fits into the tetrahedral space between the four anvil faces. When a load is applied, pyrophyllite is forced between the anvils to form a gasket.

2 Design of the pyrophyllite tetrahedron

Holes of 6·35 mm diameter, passing through the centroid of each triangular face, are drilled perpendicularly to the respective faces so that they meet at the centre of the tetrahedron. Molten bismuth is poured into the resulting void and allowed to solidify. Fresh holes of diameter 5·00 mm are then drilled to leave the original holes lined with a thin layer of bismuth. Two of these holes are opened up again for the insertion of the optical windows, the outer optical surfaces of which are arranged to be just proud of the surface of the tetrahedron. The remaining space in the system is filled with optically clear cylindrical pellets of KCl, KBr or NaCl, the precise arrangement depending upon the nature of a particular experiment. The sample under investigation is usually positioned at the centre of the tetrahedron and is surrounded by a finely powdered dry alkali halide.

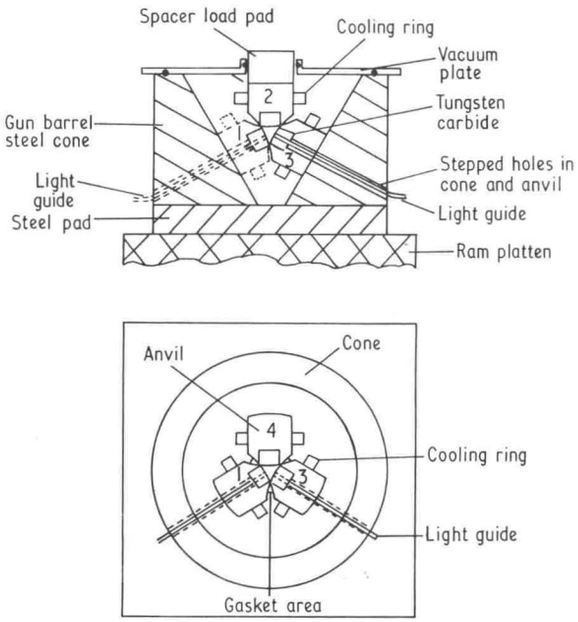

Figure 1 Schematic plan and section of a tetrahedral anvil apparatus used for optical studies

Two sorts of windows have been used: (i) synthetic single crystal sapphire cylinders of diameter 6·35 mm and length 3·18 mm, with the *c* axis parallel to the cylinder axis; (ii) diamonds in the form of polished rectangular blocks of dimensions 5 mm × 5 mm × 2 mm. The window and anvil faces that are in contact must be polished flat to within 5×10^{-5} cm. This reduces the risk of cracks developing from high local strains associated with point pressure contacts. The flatness tolerance also allows the 'ringing' together of the windows and anvil, thereby preventing pyrophyllite being forced between the window and anvil, which according to Poulter (1932) induces window breakage. The windows are positioned to cover symmetrically the 3·18 mm diameter holes in the anvil faces. In this arrangement the windows are subject to an almost uniform compressive force on all sides except that in contact with the anvil. The hydrostatic component of this force helps to inhibit crack formation and propagation.

Two examples of the use of the above system are illustrated in figure 2. In order to direct the light between the entrance and exit windows, the bismuth lining is polished, and aluminized Melinex discs are positioned to prevent light from entering the nonlight path arms of the system. For the duration of an experiment, and for half an hour before the load is applied, the cone is evacuated, thus helping to remove water from the hygroscopic halide powder, and aiding the sintering of the halide powder into a clear polycrystal on applications of the load.

In order to carry out optical measurements at low temperatures, cold dry air is passed through the anvil cooling rings

† Now at Diamond Research Laboratory, De Beers Industrial Diamond Division, Johannesburg, South Africa

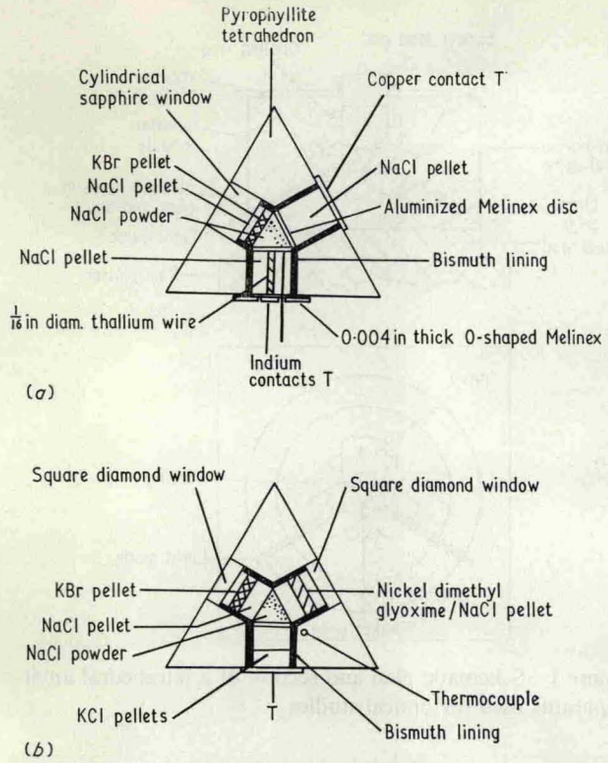

Figure 2 Schematic diagrams of tetrahedra that were used (*a*) for the determination of the bismuth and thallium calibration points, and (*b*) for the $Ni(DMG)_2$ optical calibration of the pressure

which are connected in parallel (see figure 1). The air is precooled in a series of heat exchangers using dry ice and liquid nitrogen. After passing through the cooling rings the cold air is allowed to circulate in the cone region before passing back through the initial counterflow heat exchanger. Little can be done to insulate the cone and anvil system thermally, and in consequence the consumption of dry ice and liquid nitrogen is large. Specimen temperatures within the tetrahedron as low as 100 K can be achieved and held constant to ± 5 K for several hours. Temperature measurements are made using a Chromel–Alumel Thermocoax which passes into the tetrahedron through one of the gaskets between a pair of anvils.

In a measurement of optical absorption, light from a 150 W quartz–iodine lamp is mechanically chopped at 800 Hz and focused on to the end of a 3·18 mm diameter light guide. The guide is bent so that the end protruding from the cone is horizontal, whilst the other end is adjacent to the high pressure window in the tetrahedron. Light emerging from the exit window traverses a second light guide and is then focused on to the entrance slit of a grating monochromator. The conventional exit slit of the monochromator may be replaced by an oscillating slit of constant width, the amplitude of vibration being variable. With the exit slit stationary, a transmission spectrum is recorded using a cooled photomultiplier and a conventional amplifier and phase-sensitive detector system. First and second derivative spectra are obtained by oscillating the exit slit and using the system adequately described elsewhere by Evans and Thompson (1969).

For work in the visible spectrum, commercially available incoherent multifibre glass guides were found to be excellent and preferable to single fibre guides. Although the latter have a greater intrinsic transmission, they suffer badly from surface damage as they are inserted into the cone and anvils. For work in the ultraviolet spectrum a Spectrosil quartz rod was coated by repeated vacuum evaporation with a uniform layer of LiF which in turn was covered with a layer of shellac for protection.

3 Pressure calibration at room temperature

A knowledge of the pressure acting on a sample for a given load is essential for the interpretation of high pressure experiments. For a tetrahedral anvil apparatus there is no simple 'force divided by anvil area' relationship, because of the unknown properties of the load that is supported by the gaskets. Also the compressibilities of the substances making up the volume of the tetrahedron have an important effect on the load–pressure relatonship (Lees 1966). The pressure calibration relies on the detection during each experiment of one or more of the phase transitions shown in table 1.

Table 1 Phase transitions of the materials used for pressure calibration

Phase transition	Associated physical change	Pressure characteristic of phase change (kbar)		Literature reference
		198 K	150 K	
KBr: FCC → BCC	10·5% volume decrease	17·9	19·5†	Bridgeman 1940
KCl: FCC → BCC	11% volume decrease	19·4	20·3†	Bridgeman 1940
Bismuth I → II	5% volume decrease 83% resistance decrease	25·3	NP	Il'ina and Itskevich 1966
Bismuth II → III	3% volume decrease 100% resistance decrease	26·8	NP	Il'ina and Itskevich 1966
Bismuth 'electronic'	—	NP	28·5	Il'ina and Itskevich 1966
Bismuth I → III	Resistance decrease	NP	32·3	Il'ina and Itsckevich 1966
Thallium II → III	1% volume decrease 30% resistance increase	37	?	Kennedy and La Mori 1962
Barium II → III	2% volume decrease 25% resistance increase	59·6	?	Kennedy and La Mori 1962
Bismuth V → VI	1·5% volume decrease	81	?	Giardini and Samara 1965

† Based on a linear extrapolation of data at higher temperatures. NP, transition not observed under the conditions quoted. ?, no information appears to be available.

Schematic plans of typical tetrahedra used for calibration are shown in figure 2. The electrical resistance between the two contact tabs labelled T depends upon the resistances of bismuth and thallium components, and these increase with increasing pressure at constant temperature. The bismuth I → III, bismuth II → III and thallium II → III transitions show up as slope discontinuities in the measured resistance. As the resistance of the bismuth and thallium is small, measurements are made with an AC Kelvin double bridge. The off-balance potential of the bridge is detected and continuously monitored using an amplifier and phase-sensitive detection system. Changes of the order of $10^{-6}\ \Omega$ can be detected with ease, providing ample sensitivity for the detection of the transitions.

Also placed in the light path in the tetrahedron was a small KBr disc. The transition of the KBr from its FCC to its BCC structure at a hydrostatic pressure of 18 kbar is detected directly by observing a large discontinuity in optical transmission, and indirectly by a bismuth resistance discontinuity. This latter discontinuity is caused by the 10% volume change of the KBr, resulting in strains and permanent distortion of the surrounding bismuth layer.

The nonlinearity of the load–pressure relationship necessitates a measurement of the pressure between the fixed points obtained by the detection of the various phase transitions. This is done by studying the pressure induced shift of the absorption peak at 19 000 cm^{-1} (see Zahner and Drickamer 1960) in nickel dimethylglyoxime ($Ni(DMG)_2$), and comparing the results obtained with calibration results of Davis (1968). Some examples of room temperature calibration curves using $Ni(DMG)_2$ are given in figure 3. Curve A represents the calibration for a tetrahedron containing a large quantity of KBr, and curve B is for one containing a small quantity of KBr, the remaining voids being filled with NaCl. The two sets of data diverge above the KBr phase transition, and this is attributed to the pressure-dropping effect of the KBr volume change. The curves amply demonstrate that there is not a linear load–pressure calibration in the region of a large volume change in any high pressure apparatus which relies on gaskets to support the pressure. It is also seen that above and below about 10 kbar the load–pressure curve has different slopes.

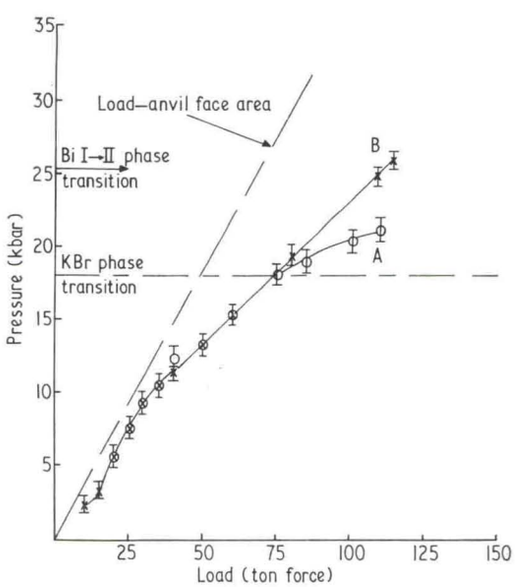

Figure 3 Room temperature pressure calibration curves. Curve A gives results when the tetrahedron contained a large quantity of KBr and curve B results when the tetrahedron contained a small quantity of KBr

4 Pressure calibration at low temperature

To obtain fixed points on the calibration curve for experiments below room temperature, the phase transitions of KBr, KCl and Bi were used. The temperature dependence of the KBr and KCl transitions have been studied down to dry ice temperature by Bridgeman (1940) and a linear extrapolation has been used in the present work for lower temperatures. The low temperature phase diagram of bismuth has been studied by several authors (Il'ina and Itskevich 1966, Roux *et al.* 1969). There is some dispute in the literature as to the existence of the transition that Il'ina and Itskevich see at low temperatures and regard as an 'electronic' rather than a crystallographic phase transition. Roux *et al.* (1969) do not see this transition.

Results during an experiment at 140 K are shown in figure 4. The experimental arrangement inside the tetrahedron was that indicated in figure 2(*b*). The region from 0 to 100 ton force is characterized by a steady decrease in optical transmission (see figure 4(*a*)), probably caused by the fracture of the clear halide discs due to distortions in the tetrahedron. This effect

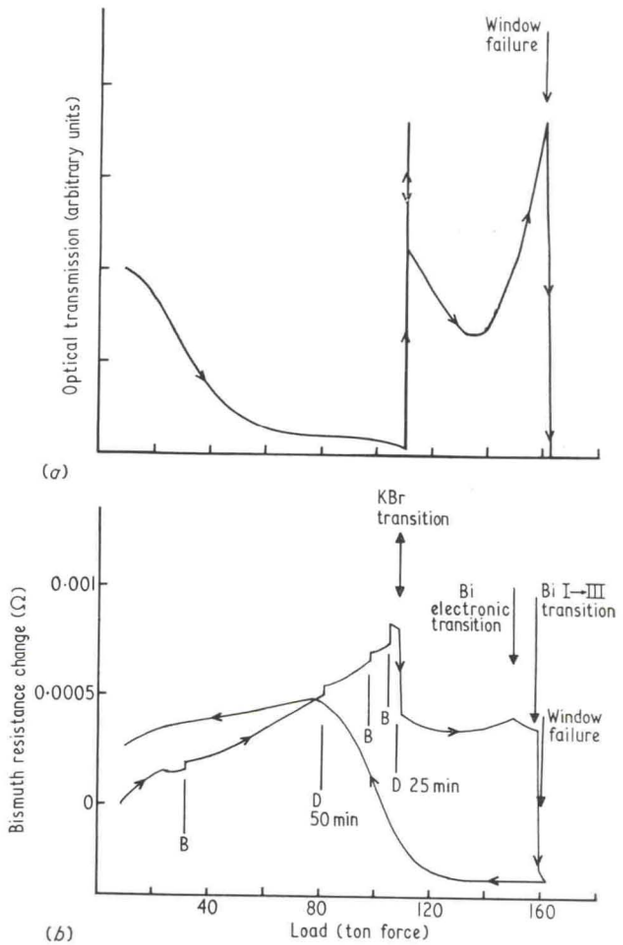

Figure 4 The upper curve shows a typical variation of optical transmission as the load is increased. The KBr phase transition and catastrophic window failure are indicated on the diagram. The lower curve shows the typical behaviour of the resistance of the bismuth, the KBr, Bi 'electronic' and Bi I → III phase changes as indicated. The results were recorded at 140 K

is greater in the low load region where the gaskets undergo the largest changes.

The KBr transition at about 108 ton force is marked by a large increase in optical transmission. The applied load was kept constant at 108 ton force for 25 min. During this time the transmission increased to a maximum after 10 min, and then steadily decreased. Such an increase in transmission was not seen by Wiederhorn and Drickamer (1960) when they investigated the phase transitions in various potassium halides. Instead a sudden decrease in signal was reported. The KBr and KCl discs used in the present experiments were formed by cold compaction of the powder, whereas Wiederhorn and Drickamer used single crystal material. The discs of the present work had a slightly milky appearance caused by light scatter from voids in the polycrystalline matrix. At the phase change these voids fill and also the interfaces (such as the KBr–window interfaces) improve to give a decrease in light scattering. The multiple nucleation of the BCC high pressure phase of KBr results in grain boundary scattering and causes a decrease in transmission, but this is later followed by an increasing transmission as grain growth proceeds.

The variations with pressure of the bismuth resistance which accompany the above optical effects are shown in figure 4(*b*). The load was increased at intervals of 2 ton weight with pauses of duration of the order of 10 min between each increment. Over most of the range the bismuth resistance increases monotonically. At the points labelled B, discontinuous increases in resistance were recorded and were accompanied by a noise from the apparatus as gaskets adjusted to the new loading conditions. At the points labelled D, the resistance discontinuities show the changes in resistance at constant load during the periods indicated. Most of these changes occur within a few minutes, and thereafter the system remains stable. The Bi I → III transition shows clearly at 160 ton force. A change in the slope of the resistance curve is also indicated at about 152 ton force, and may be related to the 'electronic' phase transition mentioned by Il'ina and Itskevich (1966). Following a window failure at 164 ton force the load on the cell was relieved. It is found that even without window failure, the pressure calibration of the system is not the same when loading and unloading the system.

Using the tetrahedron design shown in figure 2(*b*) the load dependence of the absorption peak in $Ni(DMG)_2$ was measured at low temperatures. The results are shown in figure 5. The apparatus was cooled down from room temperature to 130 K at a load of 20 ton force. Then, while the temperature was maintained constant to ±7 K, the load was increased and the peak position monitored. It is presumed that most of the energy shift of the peak at the load of 20 ton force derives from the temperature change from 293 to 130 K rather than from changes at hydrostatic pressure due to cooling. The justification for believing this is that a similar energy shift for the band is observed at ambient pressure if the same temperature variation is applied.

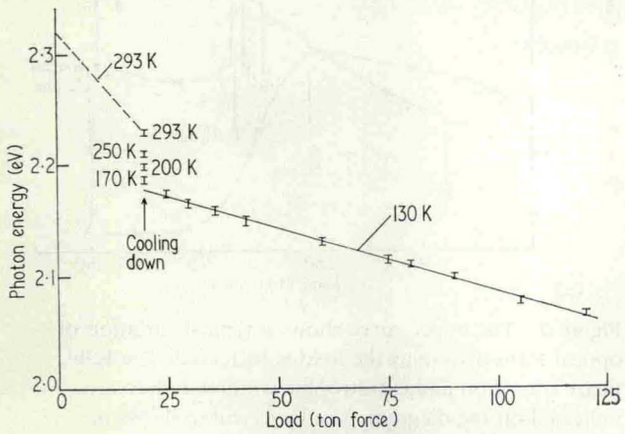

Figure 5 The load dependence of the optical absorption peak in $Ni(DMG)_2$ at 130 and 293 K

The results of figure 5 show that the energy E_{130} of the absorption peak in $Ni(DMG)_2$ at 130 K is given by

$$E_{130}(p) = A + KL \tag{1}$$

where A and K are constants and L is the applied load. The KBr transition in this run occurred at 140 ton force.

If the assumption is made that the pressure shift of the $Ni(DMG)_2$ absorption peak has a similar form at low and room temperatures, then, following Davis (1968),

$$E_{130}(p) = E_{130}(p=0) + c_1 p + c_2 p^2 \tag{2}$$

where c_1 and c_2 depend upon temperature and p is the hydrostatic pressure.

Eliminating $E_{130}(p)$ from (1) and (2) gives

$$p = \{A - E_{130}(p=0)\}/c_1 + KL/c_1 \quad \text{if } c_2 \ll c_1. \tag{3}$$

At ambient pressures Davis (1968) finds $c_1 \sim 100\, c_2$.

As equation (3) represents a linear dependence of p upon L, the relationship is determined by measuring (i) the applied loads at which the Bi and KBr phase transitions occur and (ii) the energy of the $Ni(DMG)_2$ peak at the point A in figure 5, from which the hydrostatic pressure can be inferred from the room temperature calibration of Davis (1968).

5 Limitations and applications

The size of the apparatus limits its usefulness. Experiments have to be built around the press rather than vice versa. Its bulk also limits the minimum obtainable temperature and hence the diversity of permitted experiments.

The maximum obtainable pressure is limited by the breaking strain of the windows. Pressures as high as 50 kbar have been achieved. In all experiments in which the maximum pressure obtained is greater than about 5 kbar the sapphire windows are found to be cracked at the end of the experiment. The cracking is detected by a sharp reduction in the cell transmission which occurs typically at 35 ton force as the load is reduced from, say, 150 ton force (i.e. 30 kbar at 25°C). The window contains cracks throughout the entire cylinder.

At high pressures (e.g. 25 kbar) and low temperatures (e.g. 150 K) catastrophic window failure sometimes occurs, resulting in a very large reduction in transmission. The window is damaged in a different manner from that described above. The circular area near the hole in the anvil is powdered to a depth of about 1 mm. The corresponding area on the high pressure side of the window contains a triangular dimple, the apex of which is about 1 mm below the surface. The whole high pressure surface is perfectly smooth and suggests that some form of plastic deformation may have occurred. The crack density in the bulk of the window is high. Many cracks extend throughout the crystal on planes perpendicular to the cylinder axis, i.e. along the basal planes of the sapphire.

Experiments which involve the measurement of optical density are not easily carried out with the present system because of the large number of optical components in the light path. Difficulties arise on account of relative motions of one component with respect to another, resulting in changes in the overall transmission of the system. The apparatus has been used very successfully to measure the changes in energy of optical absorption lines which are clearly resolved.

Table 2 The pressure dependencies of five zero phonon absorption lines found in diamonds, in the range 0–30 kbar

Energy of absorption line (eV)	1·673	2·087	2·464	2·497	2·987
Wavelength of absorption line (nm)	741·0	594·0	503·2	496·5	415·2
Hydrostatic shift (10^{-4} eV kbar^{-1})	$0·4 \pm 0·3$	$6·5 \pm 0·1$	$3·9 \pm 0·1$	$3·9 \pm 0·4$	$1·8 \pm 0·4$

The pressure dependencies of five zero phonon lines in diamond have been measured at 130 K in the pressure range 0–30 kbar and the results are summarized in table 2. The half-widths of these lines are of the order of 0·01 eV. Detailed discussion of these results will appear elsewhere. Measurements have been made also on an absorption band at 3·19 eV in lithium iodide at 150 K, (in this case the halfwidth is about 0·7 eV at 295 K) giving a linear energy shift in the range 0–19 kbar, $(\partial E/\partial p)_{150K} = 0·013 \pm 0·001$ eV. The apparatus is also suited to the measurement of the effects of hydrostatic pressure on the energies of fluorescence emission and Raman scattering excited by laser radiation.

6 Summary

It has been shown that a tetrahedral anvil apparatus can be modified with relative ease to allow optical experiments to be carried out on large samples at temperatures down to about 100 K and at pressures in the range 0–50 kbar. Pressure calibrations differ when the design of the pyrophyllite tetrahedron are not the same, but are consistent in different runs using the same arrangements. Phase transitions appear to be very well defined, indicating that the hydrostatic pressure in the alkali halide medium is reasonably homogeneous. The fact that the various methods of pressure calibration are consistent also support this view.

Acknowledgments

We acknowledge the financial assistance provided by De Beers Industrial Diamond Division and by The Science Research Council. We are indebted also to our colleagues R G Artus, A Priest, D Prince and R A Winters for their patient technical assistance and for help in experimentation.

References

Bradley C C 1969 *High Pressure Methods in Solid State Research* (London: Butterworth) p 78

Bridgeman P W 1940 *Proc. Am. Acad. Arts Sci.* **74** 21

Davis H W 1968 *J. Res. Nat. Bur. Stand.* **72A** 149

Evans B L and Thompson K T 1969 *J. Phys.* E: *Sci. Instrum.* **2** 327

Giardini A A and Samara G A 1965 *J. Phys. Chem. Solids* **26** 1523

Il'ina M A and Itskevich E S 1966 *Sov. Phys. – Solid State* **8** 1873

Kennedy G C and La Mori P N 1962 *J. Geophys. Res.* **67** 851

Lees J 1966 *Adv. High Press. Res.* **1** 2

Poulter T G 1932 *Phys. Rev.* **40** 860

Roux C, Andreani M and Rapin M 1969 *Coll. Int. Propriétés Phys. des Solides sous Pression, Grenoble* (Paris: CNRS) p 447

Wiederhorn S and Drickamer H G 1960 *J. Appl. Phys.* **31** 1665

Zahner J C and Drickamer H G 1960 *J. Chem. Phys.* **33** 1625

Journal of Physics E: Scientific Instruments 1973 Volume 6